Electronic Supplementary Material (ESI) for Industrial Chemistry & Materials.

Flexoelectricity in hydroxyapatite for enhanced piezocatalytic degradation of phenanthrene in soil

Jun Han, Wenrou Tian, Ye Miao, Najun Li,* Dongyun Chen, Qingfeng Xu, Hua Li and Jianmei Lu*

College of Chemistry, Chemical Engineering and Materials Science, Collaborative Innovation Center of Suzhou Nano Science and Technology, Soochow University, Suzhou 215123, China

**Correspondence to: J. M. Lu (E-mail: lujm@suda.edu.cn) and N. J. Li (E-mail: linajun@suda.edu.cn), Tel.: 86 512 65880368*

Supporting Information

Table S1 The parameters of GC-MS test for PHE concentration in soil

Gas Chromatography	
Injector temperature	280 °C
Injection volume	1.0 μL
Gas flow rate	1.0 mL min^{-1}
Column temperature	80 °C for 2 min; raised to 180 °C at rate of 20 °C min^{-1} for 5 min; finally, raised to 290 °C at rate of 10 °C min^{-1} for 5 min.

Mass Spectrometer (Selective Ion Mode)	
Ion power temperature	230 °C
Ionization energy	70 eV
Interface temperature	280 °C
Quadrupole temperature	150 °C
Mass scan range	45-450 amu
Solvent delay time	5 min

Table S2 the F content of different catalysts

	HAP@FAP-0.5	**HAP@FAP-1**	**HAP@FAP-1.5**	**HAP@FAP-2**	**F(1.5)-HAP**
Concentration of NaF	2 mM	4 mM	6 mM	8 mM	6 mM
F	7.30	8.48	10.25	10.75	13.52
Ca	92.40	90.52	89.75	89.25	86.48
F : Ca	8.23%	10.47%	11.42%	11.98%	15.63%
Feeding ratio	5%	10%	15%	20%	15%

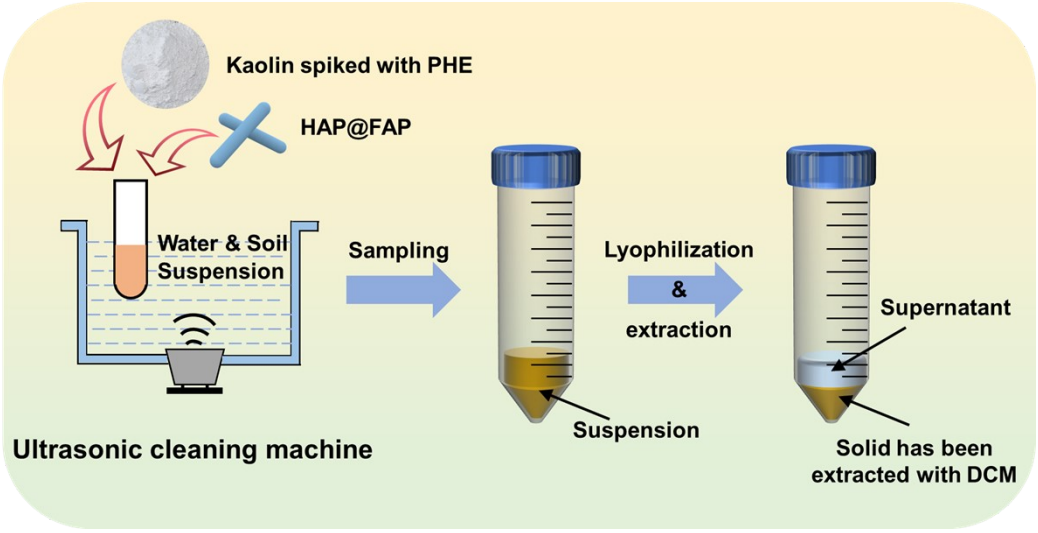

Fig. S1 The schematic diagram of the piezocatalytic degradation experiment.

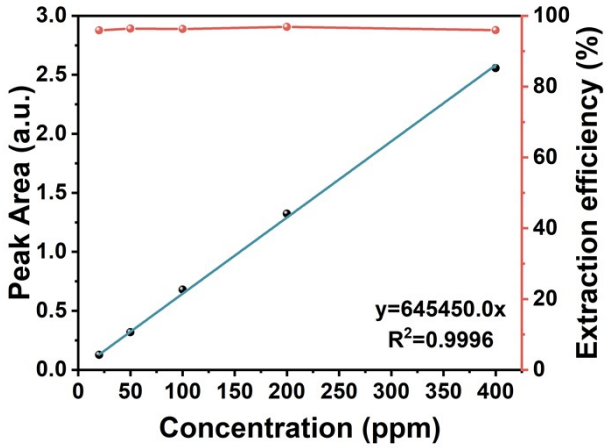

Fig. S2 Standard curve and extraction efficiency of PHE from soil.

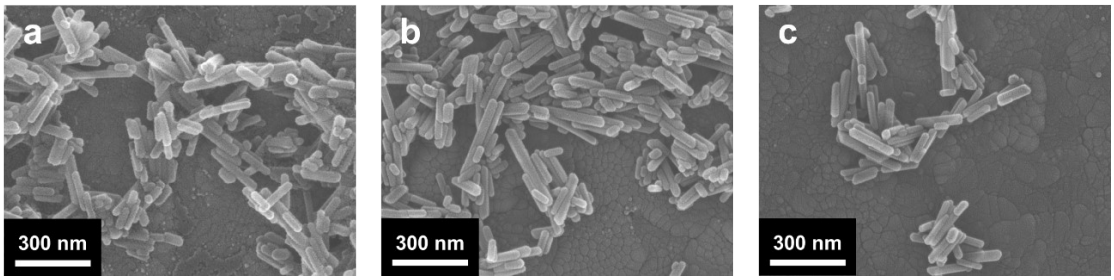

Fig. S3 SEM images of (a) HAP@FAP-0.5; (b)HAP@FAP-1 and (c) HAP@FAP-2.

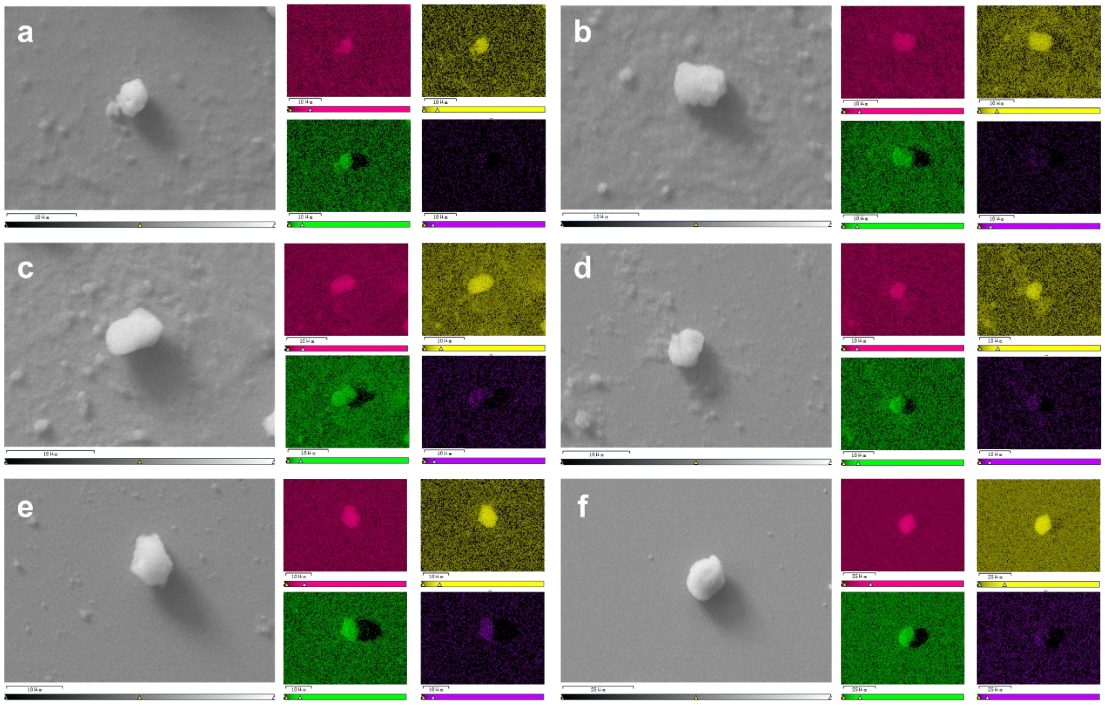

Fig. S4 EDS mapping of (a) HAP; (b) HAP@FAP-0.5; (c) HAP@FAP-1; (d) HAP@FAP-1.5; (e) HAP@FAP-2 and (f) F(1.5)-HAP (Scale bar: 10 μm. Pink, Ca element; yellow, P element; green, O element; purple, F element).

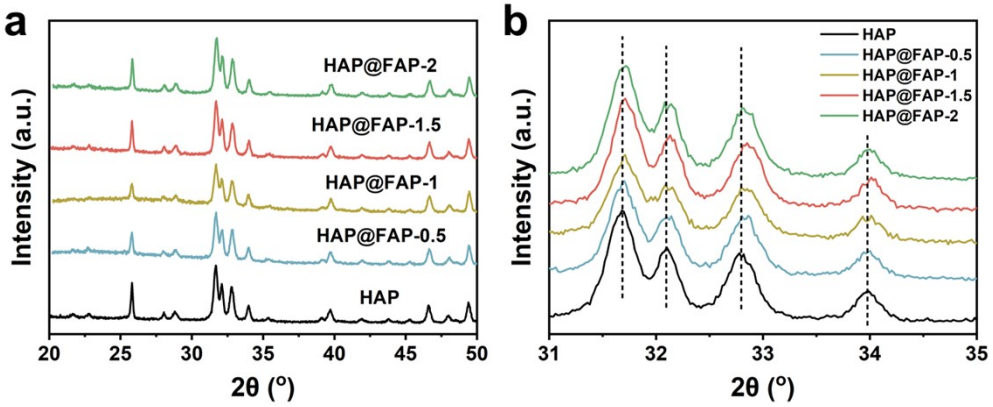

Fig. S5 The XRD pattern of (a) HAP and HAP@FAP-x; (b) its enlargement between 31-35°.

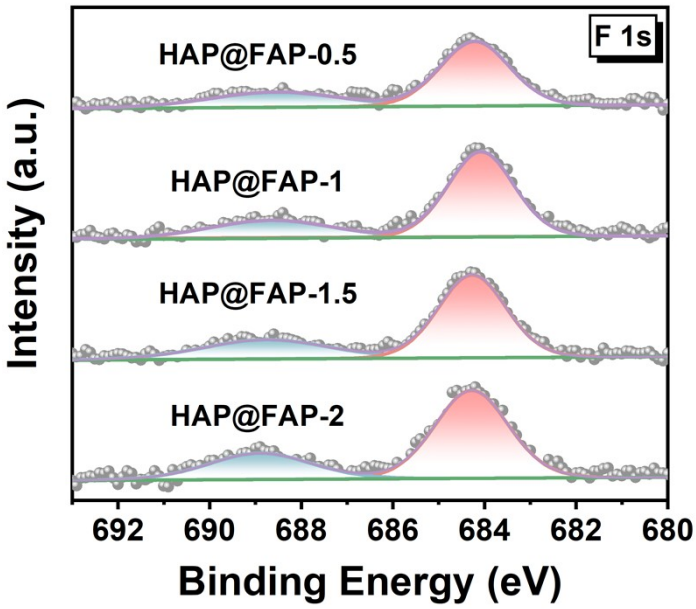

Fig. S6 F 1s high-resolution XPS spectra of HAP@FAP-x (x=0.5-2).

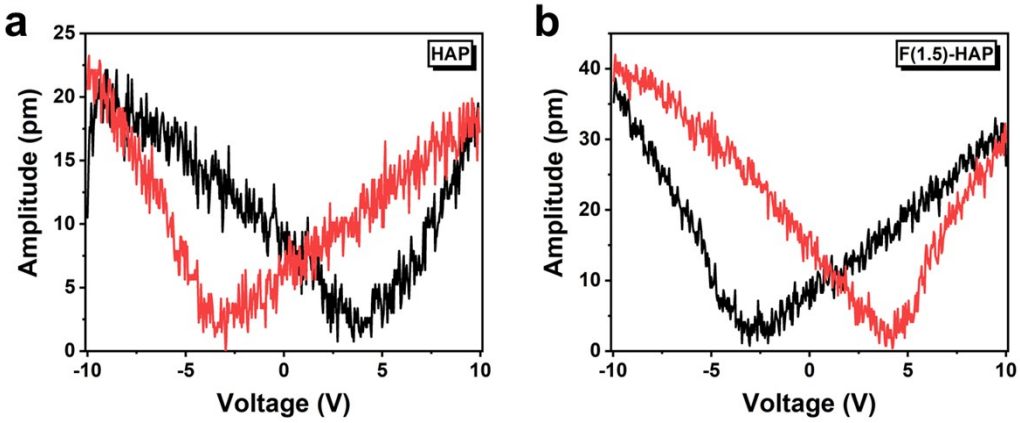

Fig. S7 PFM amplitude diagram of (c) HAP and (b) F(1.5)-HAP.

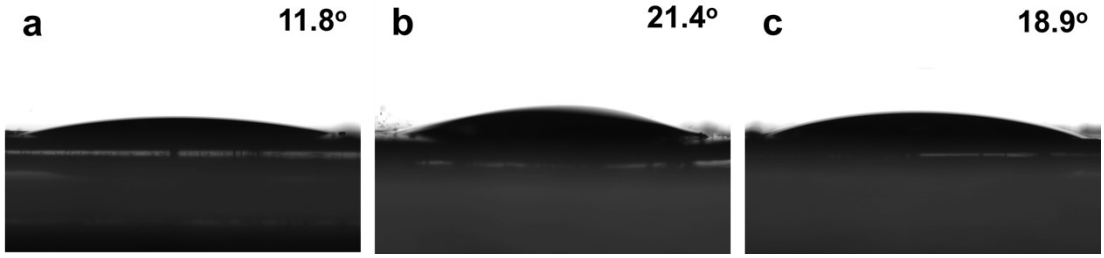

Fig. S8 The water contact angle of (a) HAP; (b) HAP@FAP-1.5 and (c) F(1.5)-HAP.

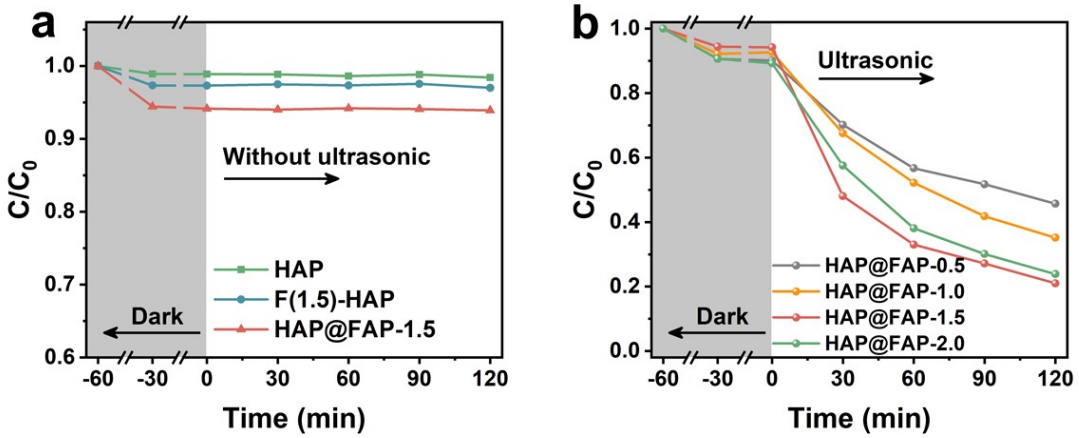

Fig. S9 (a) the degradation efficiency of PHE by HAP, F(1.5)-HAP, HAP@FAP-1.5 without ultrasonic and (b) HAP@FAP-x with gradient F-doping.

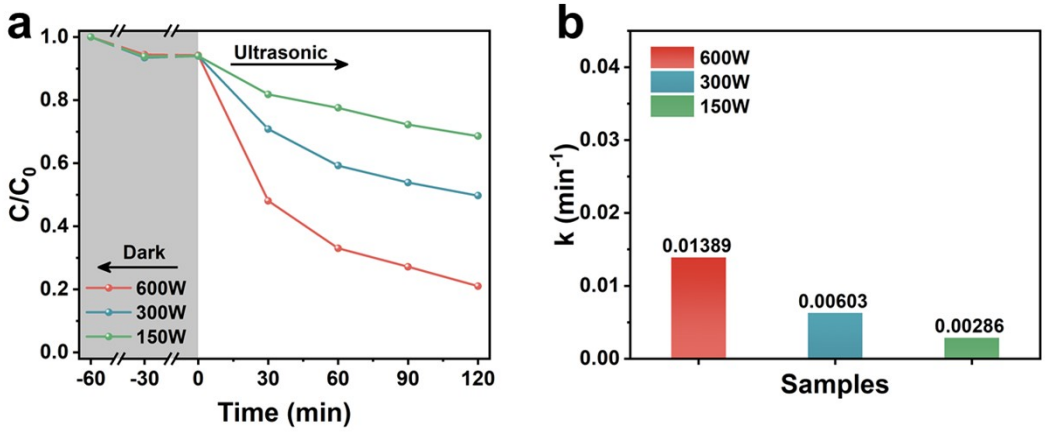

Fig. S10 (a) the degradation efficiency of PHE by HAP@FAP-1.5 under different ultrasonic powers and (b) the corresponding degradation kinetic rate constants (min^{-1}).

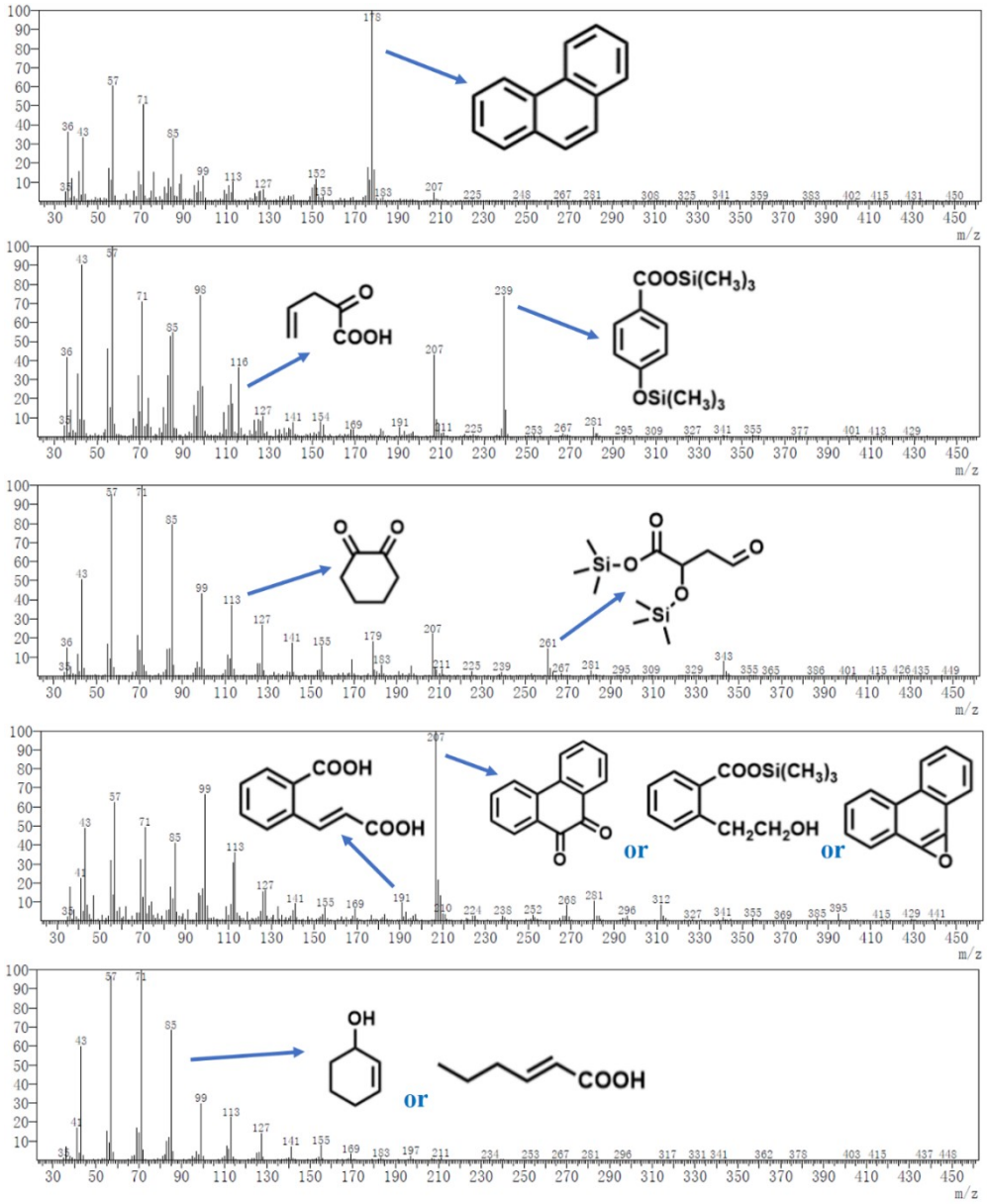

Fig. S11 The GC-MS results of intermediates in the degradation of PHE.

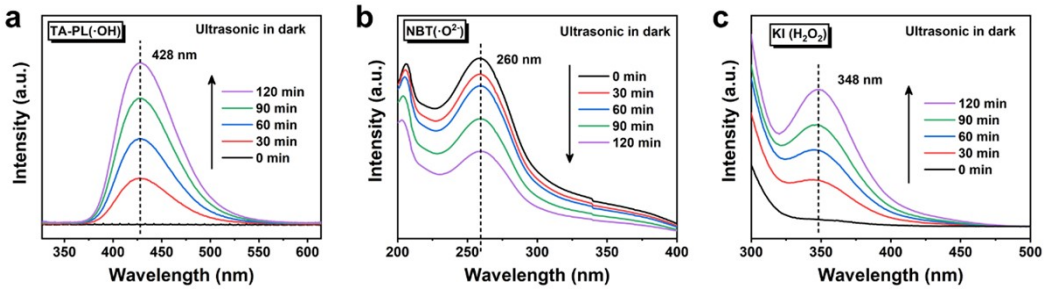

Fig. S12 (a) TA-PL; (b) NBT transformation and (c) iodide method under ultrasonic to detect ·OH, $\cdot O_2^-$ and H_2O_2 produced by HAP@FAP-1.5 under ultrasonic.